Comparison of monopolar and bipolar diffusion weighted imaging sequences for detection of small hepatic metastases(Dissertation_全文)

AUTHOR(S):

Furuta, Akihiro

European Journal of Radiology

Comparison of monopolar and bipolar diffusion weighted imaging sequences for detection of small hepatic metastases

Akihiro Furuta, MD,[1] Hiroyoshi Isoda, MD, PhD,[1] Rikiya Yamashita, MD,[1] Tsuyoshi Ohno, MD,[1] Seiya Kawahara, MD,[1] Hironori Shimizu, MD,[1] Toshiya Shibata, MD, PhD,[1] Kaori Togashi, MD, PhD,[1]

[1]Department of Diagnostic Imaging and Nuclear Medicine, Kyoto University Graduate School of Medicine

Address correspondence to: Akihiro Furuta MD.

Department of Diagnostic Imaging and Nuclear Medicine, Kyoto University Graduate School of Medicine, 54 Kawahara-cho, Shogoin, Sakyo-ku, Kyoto 606–8507, Japan.

Tel.: 81-75-751-3760 Fax: 81-75-771-9709

Comparison of monopolar and bipolar diffusion weighted imaging sequences for detection of small hepatic metastases

OBJECTIVE:

To compare monopolar (MP) and bipolar (BP) diffusion weighted imaging (DWI) in detecting small liver metastases.

MATERIALS AND METHODS:

Eighty-eight patients underwent 3-T MRI. The signal-to-noise ratios (SNR) of the liver parenchyma and lesions, the lesion-to-liver contrast-to-noise ratios (CNR), and the detection sensitivities were compared. The lesion distortion was scored (LDS) from 4 (no distortion) to 1 (excessive distortion), dichotomised as no-distortion and distortion, and the association between detected lesions for each reader in the MP or BP DWI group and the dichotomised lesion distortion degree was assessed.

RESULTS:

Forty-six hepatic metastases were confirmed. The CNR with BP images showed significantly higher values than with MP ($P = 0.017$). The detection sensitivities of the three readers were higher in the BP sequence than in MP, and one reader detected significantly more hepatic lesions with BP images ($P = 0.04$). LDS was significantly improved with BP sequence ($P = 0.002$). In the no-distortion group, excluding the MP DWI assessments of one reader, detection sensitivities were significantly higher than in the distortion group ($P < 0.001$ and $P = 0.002$, respectively).

CONCLUSION:

Reduced lesion distortion improves the detection of small liver metastases, and BP is more sensitive in detecting small liver metastases than MP DWI.

Keywords: Diffusion weighted imaging, liver metastases, image quality, distortion, artefact, eddy currents

Introduction

Diffusion-weighted imaging (DWI) has the potential to differentiate and evaluate liver tumours based on the high contrast between abnormal and normal tissue. DWI can direct the radiologist to findings that may otherwise be overlooked (1). Gadolinium-ethoxybenzyl-diethylenetriamine pentaacetic acid (Gd-EOB-DTPA)- or mangafodipir trisodium-enhanced magnetic resonance imaging (MRI) reportedly show higher accuracy in detecting small hepatic metastases than does DWI, but the addition of DWI is useful (2-4).

The liver has a short T2 and low signal-to-noise-ratio, and as a result, the diffusion encoding gradients must be performed in the shortest possible echo time. A single Stejskal-Tanner monopolar (MP) sequence refocusing pulse can further shorten the echo time. However, unbalanced MP gradients can generate stronger eddy current–induced distortions at high b-values (5). In a previous liver diffusion study, a twice-refocused bipolar (BP) diffusion preparation was used (6) and featured intrinsic low eddy current artefacts, while BP showed a longer echo time than MP sequence.

Previous studies compared the image quality and intravoxel incoherent motion in normal liver between MP and BP DWI. However, a direct comparison between the two different DWI sequences in detecting hepatic metastases has not been performed. The present study compares MP and BP sequences to determine the superior technique for detecting small hepatic metastases measuring 2 cm or less.

Materials and Methods

Patients

Eighty-eight patients underwent Gd-EOB-DTPA-enhanced MRI including DWI to detect hepatic metastasis at the Department of Radiology, Kyoto University Graduate

School of Medicine, Kyoto, Japan from January 2011 to October 2012. This retrospective study was performed in accordance with the Declaration of Helsinki (7) and approved by the local ethics committee. All patients provided informed written consent to undergo imaging examinations. Of the 88 patients, 65 were excluded as follows: concurrent chemotherapy (one patient); absent histological diagnosis and follow-up confirmation (two patients); lesions greater than 2 cm (seven patients); greater than five lesions, which can potentially be misdiagnosed as hepatic metastases (14 patients); and no hepatic metastasis (41 patients). The remaining 23 patients (16 men and 7 women, aged 41–82 years, mean age: 67 years) were included in the final analysis comprising 17 patients with colorectal cancer, four with pancreatic cancer, one with gastric cancer, and one with breast cancer.

Lesion diagnosis

Fifteen patients underwent definitive surgery with intraoperative ultrasonography (US), and 31 small hepatic metastases were histologically confirmed in these patients. In eight patients without a histopathologic diagnosis, the 15 visible small hepatic tumours were considered metastatic based on tumour growth observed at follow-up imaging examinations 3–20 months after the initial MRI. Tumour growth was defined according to Response Evaluation Criteria in Solid Tumours (RECIST) (8). Hepatic cirrhosis was not observed in any patient. The presence or absence of hepatic metastases was diagnosed by consensus between two radiologists (R.Y. and H.I., with 8 and 24 years' experience respectively, in gastrointestinal and hepatobiliary imaging) evaluating contrast-enhanced CT, US, positron emission tomography (PET) using F-18 fluorodeoxyglucose (FDG), and MRI; follow-up US, CT, FDG-PET, or MRI; and intraoperative US and serological examination. A total 46

small hepatic metastases (range: 0.3–2.0 cm; mean: 1.04 cm) in 23 patients were confirmed; five patients who did not have focal hepatic metastasis served as the control group (Table 1). Of the 23 patients, eight had solitary lesions, 10 had two lesions, and the remaining five had three or more lesions (three had three lesions, one had four lesions, and one had five lesions).

Imaging protocols

All MRI examinations were performed using a commercially available 3-T MR system (MAGNETOM Skyra; Siemens AG, Healthcare Sector, Erlangen, Germany) equipped with a spine matrix coil and body matrix coil. DWI using a single-shot spin-echo echo-planar imaging (EPI) sequence in the axial plane with respiration triggering using the PACE method (spectral presaturation with inversion recovery for fat suppression, TE = monopolar sequence: 53 ms and bipolar sequence: 69 ms, ETL = 86, ETS = 0.52 ms, slice thickness = 5 mm, gap between slices = 1.3 mm, matrix size = 86 × 128, FOV = 35 cm, number of slices = 30, b factors = 1000 s/mm^2, GRAPPA factor = 2) was acquired between the dynamic and hepatocyte phases using Gd-EOB-DTPA (Fig.1). In this study, apparent diffusion coefficient (ADC) measurement was not because it fell outside the remit of this study.

Imaging analysis

Quantitative Evaluation

Quantitative evaluations were performed by a radiologist (A.F. with 12 years' experience). Regions of interest (ROIs) were centred on the focal lesion and hepatic parenchyma using a commercially available DICOM viewer (YAKAMI Software, Kyoto, Japan) to measure signal intensity (SI) on DWI with a b-value = 1,000 s/mm^2. The ROI was constructed to maximally encompass the lesion while avoiding necrotic

cystic regions at identical sites on MP and BP sequences. Because a parallel imaging technique was employed, the background noise standard deviation (SD) could not be used to calculate the image signal-to-noise ratio (SNR); therefore, SD of the normal liver SI adjacent to the lesion was used estimate local noise (9-11). The ROI was centred in the adjacent liver parenchyma measuring at least 100 mm^2 and residing in a homogeneous portion devoid of vessels and prominent artefacts. The contrast-to-noise ratio (CNR) between the corresponding liver lesion and liver parenchyma, and the liver parenchyma or lesion SNR were calculated as follows:

$CNR = (SI_L - SI_P)/ noise$, $SNR_{parenchyma\ or\ lesion} = (SI_{p\ or}\ SI_L)/ noise$

where the liver parenchyma signal intensity is SI_P and the corresponding lesion signal intensity is SI_L. The CNR and SNR at an undetectable lesion were scored zero and one, respectively.

Qualitative Evaluation

The two patient groups (MP and BP sequences) were statistically compared. Three readers (T.O., H.S., and S.K. with 8, 10, and 10 years' experience, respectively, in gastrointestinal and hepatobiliary imaging) who were not the two diagnostic radiologists interpreted the images independently. The readers were aware of the hepatic metastasis risk but were blinded to all other historical information including the primary tumour site. All data were anonymised and randomised. Image analysis was performed on a DICOM viewer in two sessions at a 4-week interval to minimise any learning bias. Each observer recorded the presence and segmental location of the lesions based on a 5-point confidence scale: 1 = definitely not present; 2 = probably not present; 3 = equivocal; 4 = probably present; and 5 = definitely present. To accurately correlate the scored lesions and gold standard findings, each observer recorded the individual image number, segmental location, and lesion size. In single

segments containing multiple lesions, the observers recorded the lesion size and location within each segment to avoid confusion during data analysis. In addition, a radiologist (A.F.) correlated the scored lesions to a reference standard based on the recorded lesion size and location

The lesion distortion score (LDS) was assessed by two radiologists (R.Y. and H.I.) on a four-point scale from 4 (minimal or no distortion) to 1 (excessive distortion) to zero (undetected lesion). Disagreements between reviewers were resolved by discussion.

Statistical analysis

Statistical analysis was performed using Excel (2007; Microsoft Corporation, Redmond, WA, USA) with Statcel software (OMS, Tokyo, Japan).

The CNR and SNR were compared between the MP and BP groups using Wilcoxon's signed rank test. A P-value of < 0.05 was considered significant. To calculate the detection sensitivity, the presence of lesions was dichotomised. Lesions scoring 1 or 2 were "not present," and lesions scoring 3–5 were "present." The lesion detection rates were compared using the related-samples McNemar test for each reader.

Distortion was compared between the MP and BP sequence datasets with the non-parametric Wilcoxon's signed ranks test. Correlation between the degree of distortion and the lesion detection sensitivity was performed using dichotomised LDS data: 0, 1, and 2 scores indicated distortion; and scores 3 and 4 indicated absent distortion. The association between detected lesions for each reader in the two groups and the dichotomised lesion distortion was determined using the Pearson χ^2 test.

Results

Quantitative Evaluation

The mean (SD) CNR and SNR are summarised in Table 2. The CNR with BP showed significantly higher values than did MP (P = 0.017). The $SNR_{parenchyma}$ and SNR_{lesion} were not significantly different between the two methods.

Qualitative Evaluation

Lesion detection sensitivity

The detection sensitivity for the three readers and datasets are shown in Table 3. One reader detected significantly more hepatic lesions in the BP images than in the MP images (Fig. 2). The detection sensitivities of the remaining two were higher in the BP images than the MP images, but this difference was not significant.

Lesion distortion scores

The lesion distortion scores are presented in Table 4. LDS was significantly improved in the BP group than in the MP group (P = 0.002) (Fig. 3).

Correlation between distortion and detection sensitivity

In the MP group, 30 lesions were classified as no-distortion lesions (14 scoring 4 and 16 scoring 3), and 16 were classified as distortion lesions (9 scoring 2 and 7 scoring 1). In the BP group, 39 lesions were classified as no-distortion lesions (29 scoring 4 and 10 scoring 3), and 7 lesions were classified as distortion lesions (6 scoring 2, 0 scoring 1, and 1 scoring 0).

The distortion analysis is summarised in Table 5. In all of the no-distortion groups, except the MP group of reader 3, detection sensitivities were significantly higher than in the distortion groups ($P < 0.001$–P = 0.002). The detection sensitivity with MP of reader 3 was also higher in the no-distortion group than in the distortion group, but this difference was not significant.

Discussion

Accurate detection of hepatic metastases, especially small lesions, is clinically important because it may significantly affect the therapeutic approach (12). MRI, especially single-shot EPI DWI, can obtain high lesion-to-liver contrast even without a contrast agent. Recently, abdominal DWI has become widely used in cancer patients because it provides additional information facilitating lesion detection, particularly for hepatic metastasis (13,14). In this study, hepatic DWI was performed using two approaches: an MP sequence, which shortens the echo time, and a BP sequence, which reduces the eddy current.

The present study demonstrates that there is no significant difference in the liver parenchymal SNR between MP and BP sequences. Kyriazi et al. reported that the liver parenchymal SNR was lower using the BP sequence than the MP sequence (15), but our results are consistent with those of another study that reported no significant SNR difference between MP and BP sequences (5). Although the signal intensities of liver parenchyma with BP are lower than with MP, the reduced distortion in the 3-T system decreases noise during BP sequence compared to during MP sequence. Notably, the SNR of hepatic lesions were overall superior and the CNR significantly higher with the BP sequence. Potentially, the reduced distortion of BP decreased the noise compared MP despite the lowered signal intensities in the liver parenchyma and lesion, and the CNR of the BP sequence improved as a result.

The detection sensitivity of one reader was significantly higher with the BP sequence; the other two readers showed a higher detection sensitivity with the BP compared to the MP sequence, but without statistical significance. The present study also demonstrates that reading a BP sequence improves the eddy-current-induced image distortion in small liver metastases compared to the MP sequence. For the

distortion analysis classified as no-distortion and distortion lesions by LDS, the no-distortion group detection sensitivities were significantly higher than in the distortion group, except in one reader with the MP sequence. This particular reader also had a higher detection sensitivity in the no-distortion than in the distortion group, but the difference was not significant. This result suggests that lesion distortion strongly influences the lesion detection sensitivity. Rosenkrantz et al. reported a higher sensitivity with reduced distortion DWI compared to DWI alone when detecting prostate cancer (16). In addition, the image quality of hepatic parenchyma in BP DWI is reportedly superior to that with the MP sequence by reducing the eddy-current-induced distortion (15). However, an association between the lesion distortion in DWI and lesion detection sensitivity has not been previously reported. Presumably, the hepatic lesion distortion is reduced in the BP sequence compared to the MP sequence. This may explain the distortion at the tumour-parenchyma boundary causing blurring of the lesion shape; as a result, distorted lesions may be overlooked. Chung et al. reported that the detection sensitivity of small liver metastases (≦2 cm) using DWI is lower compared to sensitivity in larger metastases (＞2 cm) (17). Although the detection sensitivity was decreased by the eddy current induced artefact in the small liver metastases (≦2 cm) targeted in the present study, the eddy-induced distortion may not influence the detection sensitivity of larger lesions (＞2 cm).

The short liver T2 requires the diffusion-encoding gradients to be set at the shortest possible echo time. Also, because the liver is a relatively homogeneous abdominal organ, it was thought that liver metastases would not be easily influenced by the eddy current-induced distortion. Therefore, the detection sensitivity with MP was expected to be higher than with BP, but the opposite relationship was observed.

Other abdominal organs have a longer T2 and more heterogeneous parenchyma than the liver; therefore, the higher metastasis detection rate with BP may be similar in other organs.

Only one lesion on bipolar DWI was not detected due to physiologic and movement-related artefacts. The lesion was very small (7 mm diameter) and located in the superior lateral lobe. In this location, images can be markedly distorted by pulmonary and intestinal air, and signal loss may be caused by cardiac motion (18, 19). This may be observed only during MP because the SI of lesions were higher on MP sequence than on BP sequence.

The study had several limitations. Being a retrospective study with a small sample size, the data may have been influenced by selection and verification biases. Further prospective studies using a larger patient population are recommended to confirm the present findings. Furthermore, not all lesions were compared and confirmed with surgical specimens. However, lesions were diagnosed using a multi-modality imaging follow-up performed by two experienced readers, which limits the risk of misclassification. Notably, 14 patients with more than five focal hepatic lesions were excluded. A relatively large number of patients were excluded, potentially leading to selection bias. DWI was acquired after administering Gd-EOB-DTPA to shorten the examination time, and this may have affected the ADC values. However, a recent paper reported that ADCs of focal hepatic lesions were not significantly different before and after contrast administration, and DWI after Gd-EOB-DTPA administration can substitute for unenhanced DWI at 3.0 T without compromising the CNR and ADC of focal hepatic lesions (20). Finally, the hepatic lesion detection and characterisation ability of these DWI sequences was not compared to other sequences because the

study only aimed to objectively compare the image quality between the two DWI sequences.

In conclusion, the BP DWI sequence reduced eddy current more than the MP DWI sequence and was acceptable in detecting small liver metastases because the detection sensitivity of small liver metastases is affected by eddy current-induced lesion distortion.

Acknowledgements

The authors thank Masato Uchikoshi (Siemens Japan K.K.) for his excellent technical assistance and advice on sequence optimization in our study.

References

1. Kele PG, van der Jagt EJ. Diffusion weighted imaging in the liver. World journal of gastroenterology 2010;16(13):1567-1576.
2. Shimada K, Isoda H, Hirokawa Y, Arizono S, Shibata T, Togashi K. Comparison of gadolinium-EOB-DTPA-enhanced and diffusion-weighted liver MRI for detection of small hepatic metastases. European Radiology 2010;20(11):2690-8.
3. Koh DM, Brown G, Riddell AM, et al. Detection of colorectal hepatic metastases using MnDPDP MR imaging and diffusion-weighted imaging (DWI) alone and in combination Eur Radiol. 2008;18(5):903-10
4. Donati OF, Fischer MA, Chuck N, et al. Accuracy and confidence of Gd-EOB-DTPA enhanced MRI and diffusion-weighted imaging alone and in combination for the diagnosis of liver metastases. Eur J Radiol. 2013;82(5):822-8.
5. Dyvorne HA, Galea N, Nevers T, et al. Diffusion-weighted imaging of the liver with multiple b values: effect of diffusion gradient polarity and breathing acquisition on image quality and intravoxel incoherent motion parameters--a pilot study. Radiology 2013;266(3):920-9
6. Reese TG, Heid O, Weisskoff RM, Wedeen VJ. Reduction of eddy-current-induced distortion in diffusion MRI using a twicerefocused spin echo. Magn Reson Med 2003;49(1):177-182.
7. No authors. World Medical Association Declaration of Helsinki: ethical principles for medical research involving human subjects. JAMA 2000;284(23):3043-5
8. van Persijn van Meerten EL, Gelderblom H, Bloem JL. RECIST revised:

implications for the radiologist. A review article on the modified RECIST guideline. Eur Radiol. 2010;20(6):1456-67

9. Choi JS, Kim MJ, Chung YE, et al. Comparison of breathhold, navigator-triggered, and free-breathing diffusion-weighted MRI for focal hepatic lesions. J Magn Reson Imaging. 2013;38(1):109-18.
10. Heverhagen JT. Noise measurement and estimation in MR imaging experiments. Radiology 2007;245(3):638-639.
11. Moon WJ. Measurement of signal-to-noise ratio in MR imaging with sensitivity encoding. Radiology 2007;243(3):908-909
12. Zech CJ, Herrmann KA, Reiser MF, et al. MR imaging in patients with suspected liver metastases: value of liver-specific contrast agent Gd-EOB-DTPA. Magnetic Resonance in Medical Sciences 2007;6:43-52.
13. Nasu K, Kuroki Y, Nawano S, et al. Hepatic metastases: diffusion weighted sensitivity-encoding versus SPIO-enhanced MR imaging. Radiology 2006;239(1):122-30.
14. Bruegel M, Gaa J, Waldt S, et al. Diagnosis of hepatic metastasis: comparison of respiration-triggered diffusion-weighted echo-planar MRI and five t2-weighted turbo spin-echo sequences. American Journal of Roentgenology 2008;191(5):1421-9.
15. Kyriazi S, Blackledge M, Collins DJ, Desouza NM. Optimising diffusion-weighted imaging in the abdomen and pelvis: comparison of image quality between monopolar and bipolar single-shot spin-echo echo-planar sequences. Eur Radiol 2010;20(10):2422-2431
16. Rosenkrantz AB, Chandarana H, Hindman N, et al. Computed diffusion-weighted imaging of the prostate at 3 T: impact on image quality and tumour

detection. Eur Radiol. 2013;23(11):3170-7.

17. Chung WS, Kim MJ, Chung YE, et al. Comparison of gadoxetic acid-enhanced dynamic imaging and diffusion-weighted imaging for the preoperative evaluation of colorectal liver metastases. J Magn Reson Imaging. 2011;34(2):345-53.

18. Holzapfel K, Eiber MJ, Fingerie AA, et al. Detection, classification, and characterization of focal liver lesions: value of diffusion-weighted MR imaging, gadoxetic acid-enhanced MR imaging and the combination of both methods. Abdom Imaging.2012;37(1):74-82.

19. Koh DM, Brown G, Riddell AM, et al. Detection of colorectal hepatic metastases using MnDPDP MR imaging and diffusion-weighted imaging (DWI) alone and in combination. Eur Radiol. 2008;18(5):903–910.

20. Choi JS, Kim MJ, Choi JY et al. Diffusion-weighted MR imaging of liver on 3.0-Tesla system: effect of intravenous administration of gadoxetic acid disodium. Eur Radiol. 2010;20(5):1052–6

Figure legends

Figure 1. Schematic sequence diagrams show diffusion preparation followed by a single-shot echo-planar imaging readout. RF= radiofrequency, TE= echo time. (a) When using MP diffusion encoding, an echo time as low as 53 ms can be achieved. (b) When using BP diffusion encoding, a minimum echo time of 69 ms is required.

Figure 2. Two small hepatic metastases from gastric cancer in a 70-year-old man. (a) BP sequence clearly shows two metastases at S7 (arrow) and S1 (arrowhead). (b) On MP, one lesion at S1 (arrowhead) is clearly visible, but the other lesion at S7 (arrow) is not clear.

Figure 3. Small hepatic metastasis at S5 from colon cancer in a 42-year-old man. (a) BP sequence demonstrates small metastasis at S5 with no distortion (arrow). (b) On MP, a small metastatic lesion at S5 is markedly distorted.

Table 1

Patient and tumour sample size and clinical characteristics.

	Number of patients	Number of lesions
Histologically proven hepatic metastases	15	31
Hepatic metastases confirmed by follow-up imaging	8	15
Patients without hepatic metastases	5	0

Of the 23 patients, 8 had solitary lesions, 10 had two lesions, and the remaining 5 had three or more lesions (3 had three lesions, one had four lesions, and one had five lesions). In total, 17 patients had colorectal cancer, 4 pancreatic cancer, one gastric cancer, and one had breast cancer.

Table 2

Mean CNR and SNR in BP and MP sequences[α]

	MP	BP
CNR	27.2 ± 19.3	34.4 ± 22.3*
$SNR_{parenchyma}$	18.8 ± 7.3	18.7 ± 6.7
SNR_{lesion}	46.0 ± 23.2	53.1 ± 25.3

[α]Mean ± SD.

CNR = $(SI_L - SI_P)$/ noise, $SNR_{parenchyma} = SI_p$/noise, $SNR_{lesion} = Sl_L$/ noise, where SI_p is liver parenchyma signal intensity, and SI_L is liver lesion signal intensity.

*Significant difference between MP and BP (P = 0.017).

Table 3

Detection sensitivity per-lesion in the three individual readers using BP and MP images.

	MP	BP
Reader 1	76.1% (35/46)	84.8% (39/46)
Reader 2*	65.2% (30/46)	78.3% (36/46)
Reader 3	71.7% (33/46)	82.6% (38/46)

*Statistically significant change (P = 0.04).

Table 4

Lesion distortion scores compared between BP and MP sequence groups[α]

MP	BP	
2.80 ± 1.03	3.39 ± 0.87	P = 0.002*

[α] Mean ± SD.

*Indicates a significant difference.

Table 5

Correlation between lesion distortion degree and detection sensitivity in BP and MP sequences.

Monopolar (MP)

	No distortion	Distortion	P Value
Number	30	16	
Lesion diameter[α]	10.6 ± 4.3 mm	10.0 ± 4.7 mm	
Reader 1	27 (90.0%)	8 (50%)	P = 0.002*
Reader 2	26 (86.7%)	4 (25.0%)	P < 0.001*
Reader 3	23 (76.7%)	10 (62.5%)	P = 0.31

Bipolar (BP)

	No distortion	Distortion	P Value
Number	39	7	
Lesion diameter[α]	10.4 ± 4.5 mm	10.3 ± 4.5 mm	
Reader 1	37 (94.9%)	2 (28.6%)	P < 0.001*
Reader 2	34 (87.2%)	2 (28.6%)	P < 0.001*
Reader 3	37 (94.9%)	1 (14.3%)	P < 0.001*

[α] Mean ± SD.

* Significant difference.

The lesion characterisation was dichotomised by the lesion distortion score: scores 3 and 4 were considered no distortion, and scores 0, 1, and 2 were considered distortion.

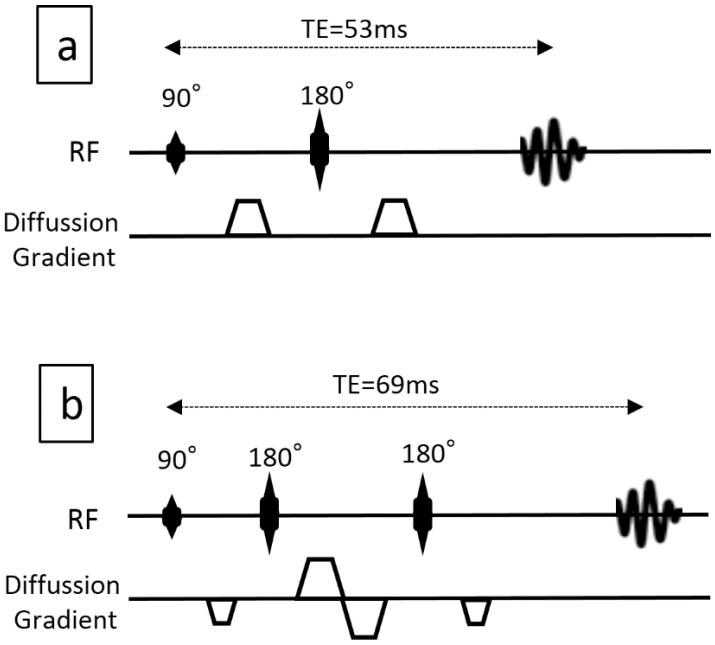

Fig. 1

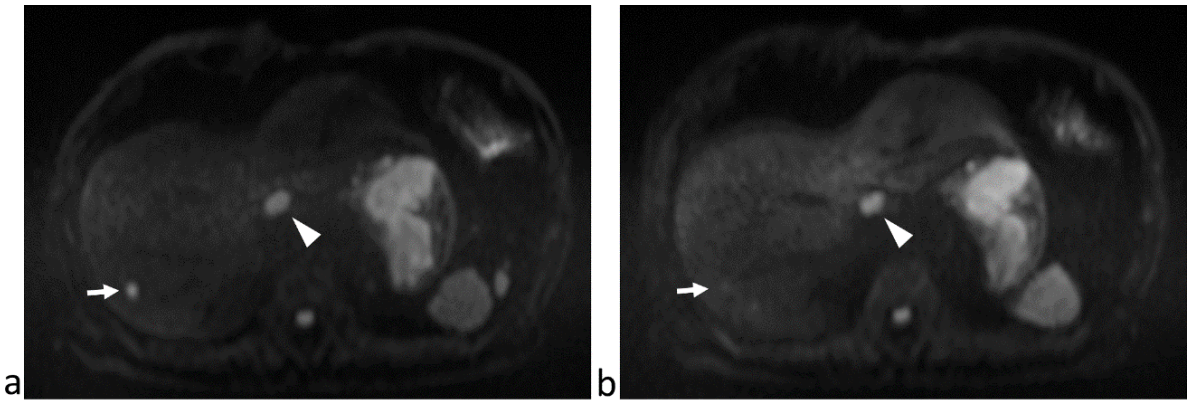

Fig. 2

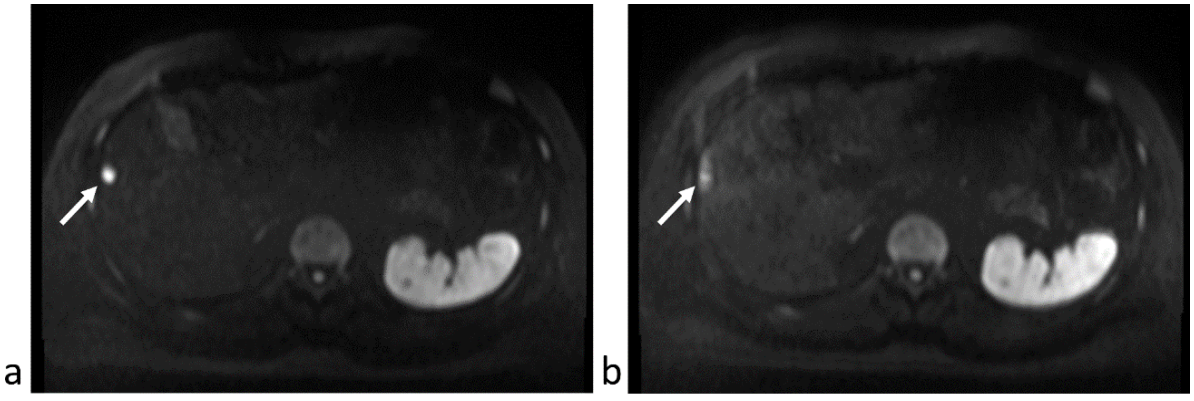

Fig. 3